

Dielectric Properties of Ultrathin SrTiO₃ and Metal-SrTiO₃ Interfaces

Bora LEE and Seungwu HAN*

Department of Physics, Ewha Womans University, Seoul 120-750

Jaichan LEE

Department of Materials Science, Sungkyunkwan University, Suwon 151-742

(Received 6 September 2007)

Using first-principles methods, we investigate the dielectric constants of free-standing ultrathin SrTiO₃ film and the dielectric response of SrTiO₃ interfaced with various metal electrodes. By examining dipole moments induced by an external electric field, we evaluate the dielectric constant of SrTiO₃ slabs with nanometer thicknesses. The dielectric constant of ultrathin SrTiO₃ is found to be substantially smaller than that of bulk SrTiO₃ and is also influenced by surface relaxation. On the other hand, the dielectric response of the metal-insulator structure shows a strong dependence on the metal electrodes; the SrRuO₃ electrode is found to interfere with the dielectric response to a lesser extent than the Pt electrode. These findings are consistent with previous experimental observations.

PACS numbers: 71.15.-m, 77.22.-d, 73.90.+f

Keywords: Dielectric constant, SrTiO₃, Ultrathin film, Metal-oxide interface

I. INTRODUCTION

As all components of microelectronic devices are scaled down to increase the integration density, several technical problems arise. A well-known issue is the leakage current through the SiO₂ gate insulator used in metal-oxide-semiconductor-field-effect transistors (MOSFET); if the performance of the down-scaled devices is to be maintained, the thickness of the gate dielectric should be reduced proportionally. According to the International Technology Roadmap for Semiconductors (ITRS), the thickness of the SiO₂ insulator will be as small as 1 nm around 2010 [1]. The leakage currents from direct tunneling in such an ultrathin SiO₂ are beyond the tolerance levels required for MOSFET devices. A possible solution is to use an alternative insulator with a higher dielectric constant, often called a high-*k* material. To date, many candidate materials, such as Al₂O₃, HfO₂, TiO₂ and SrTiO₃, have been explored. In particular, SrTiO₃ possesses the largest static dielectric constants ranging up to several hundreds at room temperature, and is considered as a material of choice to be used in an ultimately scaled device [2].

Even if high-*k* materials are employed, the material thickness is still as small as several nanometers. In those cases, it is widely accepted that the physical properties of the material can be different from the bulk properties. For example, it was observed that the dielectric

constant of SrTiO₃ is affected by the thickness of the dielectric [3,4], implying the presence of so-called intrinsic dead layers [5, 6]. This is partly attributed to the hardening of soft modes in the SrTiO₃ thin film [7]. Furthermore, the dielectric constant of SrTiO₃ is found to depend on the electrodes for the capacitor structure [8,9]. Similar observations were also reported for other high-*k* materials, such as HfO₂ [10]. The aforementioned experiments highlight that size and/or interfacial effects become significant in dielectric materials with nanoscale thicknesses. This is understandable because the ratio of the interface region to the total volume is much larger for thin films. For development of reliable electronic devices, therefore, it is important to understand how dielectric behaviors are affected by the small thickness or by interfacial structures. Experimentally, a study of ultrathin materials requires a high level of sophistication, and the interpretation is often complicated due to many coexisting origins. In this respect, theoretical studies based on the first-principles method can provide insightful information because one can systematically impose various interfacial conditions through a proper design of model structures.

In this work, we study the dielectric behaviors of ultrathin SrTiO₃ slabs and the interfacial regions of metal-SrTiO₃ junctions by using the first-principles approaches. We examine the induced dipole moments or ionic responses under external electric fields. We find that the computed dielectric constants and ionic responses are substantially different from those of the cor-

*E-mail: hanswu@ewha.ac.kr; Fax: +82-2-3277-2372

responding bulk materials and are consistent with previous experimental observations. The microscopic origins of those differences are discussed in detail.

II. COMPUTATIONAL METHOD

Throughout this work, we perform the first-principles calculations by using the PWSCF package [11] as a computational code. We employ the local density approximation to describe the exchange-correlation energies of electrons [12]. The ultrasoft pseudopotential [13] is used for the ion-electron interactions, which reduces the energy cutoff to 40 Ryd at the desired levels of convergence. The k -points on $4 \times 4 \times 1$ and $6 \times 6 \times 1$ regular meshes are used in the Brillouin zone integration for the ultrathin insulator slab and metal-insulator interface, respectively. A higher density of k -points is required to describe large electronic dispersions of the conduction electrons in metals. The atomic positions are relaxed until the Hellmann-Feynmann forces are reduced to 10^{-3} atomic units. The equilibrium lattice parameter of SrTiO₃ was calculated to be 3.85 Å, in good agreement with the experimental value of 3.91 Å [14].

SrTiO₃ can be thought of as a series of SrO and TiO₂ layers, *i.e.*, (SrO)(TiO₂)(SrO)(TiO₂)···, with each layer being electrically neutral. The dielectric constant of ultrathin SrTiO₃ is calculated following a method proposed in Ref. 15, the so-called dipole-moment method. In this method, the induced dipole moment is evaluated for an isolated slab per unit area by applying an external electric field. The slab thickness is varied, and the resulting dipole moments are linear with respect to the slab thickness. The line slope corresponds to the bulk polarization (P_{bulk}). The dielectric constant of the material (ϵ) is then calculated as follows:

$$\epsilon = \frac{\epsilon_0 E_{ext}}{\epsilon_0 E_{ext} - P_{bulk}}, \quad (1)$$

where ϵ_0 and E_{ext} are the vacuum permittivity and the external electric field, respectively. To apply the dipole-moment method to calculate the dielectric constant of ultrathin SrTiO₃, we use five different SrO-terminated slabs constructed with three to seven SrTiO₃ cubic unit cells along the z -direction which is also the direction of external electric fields. A vacuum region with a length of 20 Å is inserted within periodic supercells. The external electric fields are applied as saw-tooth potentials for compatibility with periodic boundary conditions of the plane wave basis. The dipole moments of neighboring supercells are cancelled by artificial dipole layers between supercells. Therefore, the computed dipole moments can be considered as “true” dipole moments free of the influence from other slabs [15].

On the other hand, we choose Pt or SrRuO₃ as a metallic electrode when studying the dielectric response of the metal-SrTiO₃ interface. Figure 1 shows the model

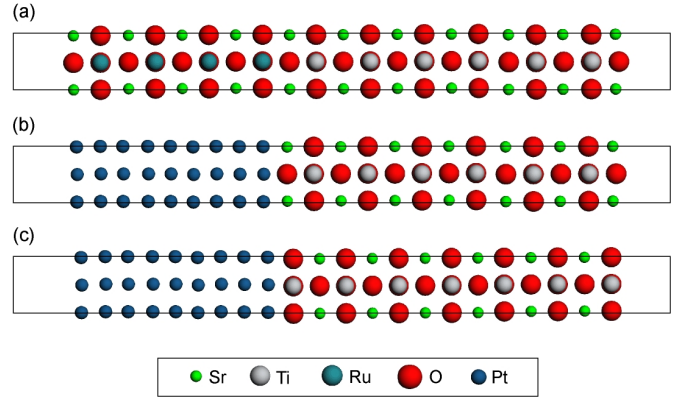


Fig. 1. Schematic model systems representing the studied metal-SrTiO₃ interfaces. (a) SrRuO₃/SrTiO₃, (b) Pt/SrO-terminated SrTiO₃ and (c) Pt/TiO₂-terminated SrTiO₃.

structures of the metal-SrTiO₃ interface. The in-plane lattice parameters of the metal electrode are adjusted to those of SrTiO₃. In the case of Pt electrodes, there are two possible types of interface, Pt/SrO and Pt/TiO₂, depending on the termination of SrTiO₃ at the interface. When an electric field is applied to the insulator slabs or the metal-oxide interfaces, we carefully confirm that there is no metal-to-insulator electron transfer, which can occur for large electric fields. This is directly checked by examining the local density of states (DOS) for the insulator slabs.

III. RESULTS

1. Dielectric Response of Ultrathin SrTiO₃ Film

Following the method outlined in the previous section, we calculate the dielectric constants of ultrathin SrTiO₃ films. Figure 2 shows the dipole moments induced in SrTiO₃ slabs with various thicknesses under an external electric field of 0.4 V/Å. We note that the electric field inside the insulator slab is the external field divided by the dielectric constants, and, as such, the internal fields are a tenth or a hundredth of the applied field. The dielectric constant can be divided into two parts - electronic and ionic responses. The electronic response dictates the optical dielectric constant (ϵ^∞) because ϵ^∞ is measured at high frequencies to which ions do not respond. Computationally, the electronic response or ϵ^∞ can be evaluated by fixing the ions at their equilibrium positions determined in the absence of the electric field. On the other hand, the static dielectric constant (ϵ^0) includes both electronic and ionic contributions; therefore, it is described by allowing all atoms to fully relax. In Figure 2, we obtain ϵ^∞ from the dashed line and ϵ^0 from the solid line, and they are 6.2 and 191.4, respectively. The optical dielectric constant compares well with the

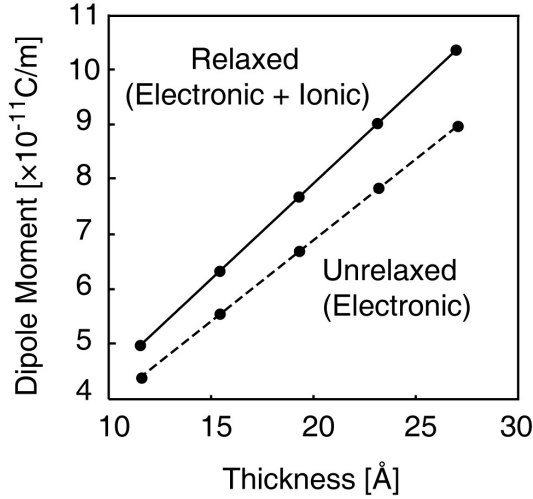


Fig. 2. Dipole moments per unit area induced in the SrTiO₃ slab with respect to the slab thickness. An external electric field of 0.4 V/Å is applied. The dashed line indicates the frozen-phonon results, and the solid line is obtained with full ionic relaxations.

experimental value of 5.6 [16]. However, the static dielectric constant is significantly different from the bulk value, as will be discussed below.

The dielectric constants of SrTiO₃ are known to strongly depend on the magnitude of the electric field, leading to a tunability property [17]. The field (E) dependence of the static dielectric constant of bulk SrTiO₃ can be formulated within the Landau-Devonshire theory as follows [18]:

$$\varepsilon(E) = \varepsilon(0) \left[1 + \left(\frac{E}{E_0} \right)^2 \right]^{-\frac{1}{3}}, \quad (2)$$

where $\varepsilon(0)$ is the dielectric constant at the zero field. From the numerical results in Ref. 18, we find that $\varepsilon(0)$ and E_0 are 391 and 14 V/ μm , respectively. By directly measuring the potential slope inside the SrTiO₃ slab, we obtain an internal field of 20.9 V/ μm . This corresponds to an external field plus depolarization field, *i.e.*, $E_{ext} - P_{bulk}/\varepsilon_0$. From Eq. (2), the expected dielectric constant of bulk SrTiO₃, in consideration of this internal field, is 264.6, which is contrasted to the measured value of 191.4 for the ultrathin SrTiO₃ in the above. This indicates that the dielectric constant of an ultrathin slab is much smaller than the bulk value, which is consistent with the experimental observations in Refs. 3 and 4.

In order to further understand the dielectric behavior of ultrathin SrTiO₃ slabs we compare two different types of boundary conditions imposed on freestanding SrTiO₃. In one case (“fixed-end”), the ions at the outermost layers are fixed to positions calculated without the external bias while in the other case (“free-end”), all ionic positions in the slab are optimized under the influence of external fields. In the above, we used the fixed-end boundary conditions for the calculation. By following the same method, we find that the static dielectric con-

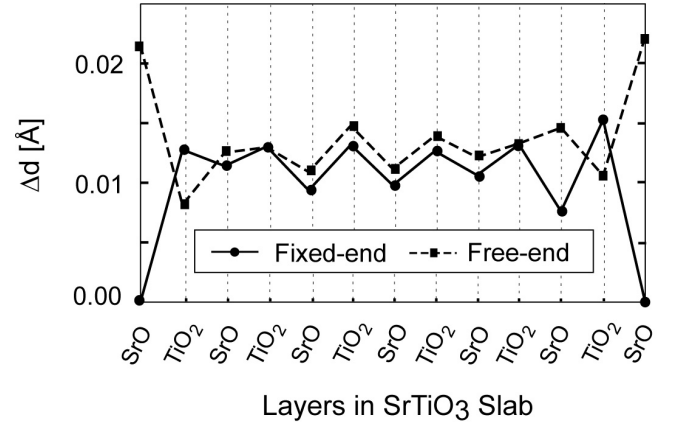


Fig. 3. Differential dipolar displacements between finite and zero fields (Δd : see text for an exact definition). The solid line is obtained by fixing atoms in the outer layer while all atoms are fully relaxed in the dashed-line data. The external field is 0.4 V/Å.

stant for the fixed-end case is only 58.9, which is less than half of the free-end value of 191.4. This implies that the ionic response of the inner layers is significantly hardened when the boundary layers are fixed. This becomes clearer by examining the differential displacement of atoms, Δd , defined as follows:

$$\Delta d = |d_{cation-anion}(E_{ext} = 0.4\text{V}/\text{Å}) - d_{cation-anion}(E_{ext} = 0\text{V}/\text{Å})|, \quad (3)$$

where $d_{cation-anion}$ means a positional differential along the z -direction between the cation and the anion in each layer. Under an external bias, the anions move along the electric field while the cations shift in the opposite direction. This displacement between anion and cation is closely related to the dipole moment of the system, which ultimately determines the dielectric constant. In Figure 3, the Δd 's at the fixed-end and the free-end conditions are compared. We find that the value of Δd in the middle layers of the fixed-end case is noticeably smaller than that for free-end condition. This is well correlated with the smaller dielectric constant for the fixed-end slab model. (We recall that the dipole-moment method extracts the dielectric constant inside the slab, so the large difference in the surface relaxation does not directly influence the computed dielectric constant).

It is an interesting question whether such a strong correlation between surface relaxation and the dielectric constant inside the slab holds for other high- k materials. As an example, we calculate the dielectric constant of a ZrO₂ (011) slab by employing the same method. The dielectric constants of ZrO₂ are 33.8 and 30.5 for the fixed- and the free-end results, respectively. That is to say, the surface relaxation does not much affect the dielectric behavior in the middle of the slab. (For comparison, 36.5 was obtained for crystalline ZrO₂ based on the Berry's phase formulation [19]). Therefore, SrTiO₃

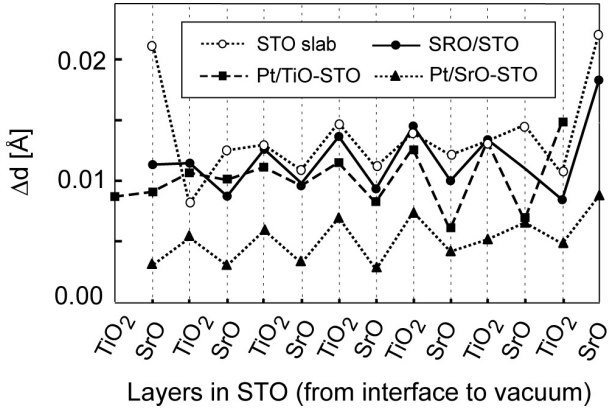


Fig. 4. Δd for three kinds of metal-SrTiO₃ (STO) interfaces. The external field is 0.4 V/Å.

is a unique material that shows an extreme sensitivity to the boundary condition.

2. Dielectric Response of the Metal-SrTiO₃ interface

The dielectric response near the metal-insulator interface is an issue that has been receiving much attention recently. The computation of the dielectric constant at the interfacial region poses many technical difficulties. With recent developments of computational methodology, a quantitative description is now feasible [20, 21]. As a first-hand analysis, we examine in this work the dielectric response at the interface, which is represented by ionic displacements. We construct various model interfaces as explained in Sec. II (see Figure 1) and apply an external electric field of 0.4 V/Å along the z -direction. In the metal-oxide interface, relative positions of valence and conduction edges with respect to the metal Fermi level should be carefully examined because the underestimation of the energy gap inherent in LDA tends to make the interface metallic. From an analysis of the local density of states [22], we find that the valence (conduction) offset of the Pt/SrO-terminated SrTiO₃ interface is 1.38 (0.60) eV while that for the Pt/TiO₂-terminated SrTiO₃ interface is 1.31 (0.57) eV. On the other hand, for the SrRuO₃/SrTiO₃ interface, the valence and the conduction offsets are 1.28 and 0.71 eV, respectively. These offsets are enough to attain insulating interfaces and surfaces as long as the applied field is not too big.

We investigate the dielectric response of the metal-SrTiO₃ interface by using local ionic displacement Δd defined by Eq. (3). Δd for each layer is plotted in Figure 4. The correlation between Δd and the actual dielectric constant was substantiated by the above study of the freestanding SrTiO₃ slab. The bigger the absolute value of the displacement is, the larger the local polarizability is expected to be along the electric field. The most interesting feature in Figure 4 is that the interfacial dielectric

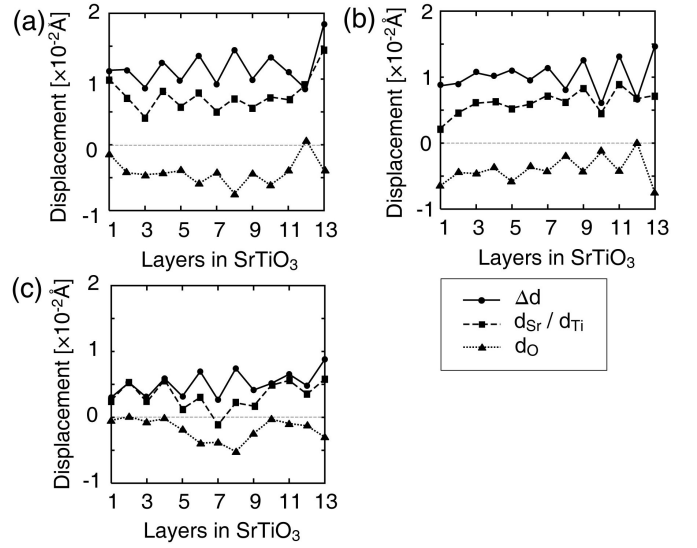


Fig. 5. Net displacement of each atom in SrTiO₃ between finite and zero fields: (a) SrRuO₃/SrTiO₃, (b) Pt/TiO₂-terminated interface, and (c) Pt/SrO-terminated interface. The solid line is Δd , which is decomposed into displacements of cations (d_{Sr}/d_{Ti} : dashed lines) and anions (d_O : dotted lines). ($\Delta d = d_{Sr}/d_{Ti} - d_O$).

response of SrTiO₃ depends substantially on the metallic electrode epitaxially attached to SrTiO₃. Δd in the middle of the slab is similar between the freestanding SrTiO₃ slab and the SrRuO₃/SrTiO₃ interface, indicating that the SrRuO₃ electrode interferes least with the intrinsic ionic motion in SrTiO₃. This is a result of the coherent crystal structures between SrRuO₃ and SrTiO₃ and is in line with the increased critical thickness reported for the SrRuO₃/BaTiO₃ interface [23]. Our results are also in good agreements with experimental finding that the dead layer is thinner when SrRuO₃ electrodes are used [24, 25]. On the other hand, the Pt electrode is found to reduce the dielectric response of SrTiO₃, particularly for Pt/SrO-terminated interface. To analyze the microscopic origin further, we plot in Figure 5 the displacement of each atom under an external electric field. It can be seen that Pt/SrO-terminated interface suppresses the displacements of oxygen atoms to near zero compared to SrRuO₃/SrTiO₃ and Pt/TiO₂-terminated interfaces. This should constitute a primary reason for the distinct dielectric behavior of the Pt/SrO-terminated interface found in Figure 4. The specific chemical bonding between Pt and O atoms could have affected the effective charges or soft phonon modes of SrTiO₃ near the interface.

IV. SUMMARY

In summary, we investigated the dielectric responses of ultrathin and interfacial structures of SrTiO₃. We found that the nanoscale ultrathin SrTiO₃ slab had a

dielectric constant substantially smaller than the bulk value. On the other hand, the dielectric response at the metal-SrTiO₃ interface showed distinct relaxation patterns depending on the types of metal electrodes and the termination of SrTiO₃. We found that SrRuO₃, rather than Pt electrodes, maintained an ionic response closer to the bulk behaviors. Our observations are all in good agreement with previous experiments.

ACKNOWLEDGMENTS

This work was supported by the Korea Science and Engineering Foundation through the Basic Research Program (Grant No. R01-2006-000-10883-0) and National Research Laboratory (NRL) program. The computations were carried out at Korea Institute of Science and Technology Information (KISTI) through the Tenth Strategic Supercomputing Program.

REFERENCES

- [1] P. S. Peercy, *Nature* **406**, 1023 (2000).
- [2] C. J. Forst, C. R. Ashman, K. Schwarz and P. E. Blochl, *Nature* **427**, 53 (2004).
- [3] C. S. Hwang, *J. Appl. Phys.* **92**, 432 (2002).
- [4] C. Basceri, S. K. Streiffer and A. I. Kingon, *J. Appl. Phys.* **82**, 2497
- [5] J. Kim, J. Pak, K. Nam and G. Park, *J. Korean Phys. Soc.* **47**, S349 (2005).
- [6] J.-Y. Kim, J.-H. Ahn, S.-W. Kang, J.-H. Kim and J.-S. Roh, *Appl. Phys. Lett.* **91**, 092910 (2007).
- [7] A. A. Sirenko, C. Bernhard, A. Golnik, Anna M. Clark, J. Hao, W. Si and X. X. Xi, *Nature* **404**, 373 (2000)
- [8] O. G. Vendik, S. P. Zubko and L. T. Ter-Martirosayn, *Appl. Phys. Lett.* **73**, 37 (1998).
- [9] M. Izuha, K. Abe and N. Fukushima, *Jpn. J. Appl. Phys.* **36**, 5866 (1997).
- [10] I. Park, T. Lee, H. Ko and J. Ahn, *J. Korean Phys. Soc.* **49**, S760 (2006).
- [11] PWSCF package is available at <http://www.pwscf.org/>.
- [12] D. M. Ceperley and B. J. Alder, *Phys. Rev. Lett.* **45**, 566 (1980).
- [13] D. Vanderbilt, *Phys. Rev. B* **41**, 7892 (1990).
- [14] H. S. Ahn, D. D. Cuong, J. Lee and S. Han, *J. Korean Phys. Soc.* **49**, 1536 (2006).
- [15] R. Ramprasad and N. Shi, *Phys. Rev. B* **72**, 052107 (2005).
- [16] I. Fedorov, *Ferroelectrics* **208**, 413 (1998).
- [17] K. H. Cho, J. Y. Ha, J. W. Choi, J. S. Kim, S. J. Yoon, C. Y. Kang and Y. P. Lee, *J. Korean Phys. Soc.* **49**, 1076 (2006).
- [18] A. Antons, J. B. Neaton, K. M. Rabe and D. Vanderbilt, *Phys. Rev. B* **71**, 024102 (2005).
- [19] D. Vanderbilt, *Phys. Rev. B* **65**, 075105 (2002).
- [20] M. Stengel and N. A. Spaldin, *Nature* **443**, 679 (2006).
- [21] B. Lee, C.-K. Lee, S. Han, J. Lee and C. S. Hwang, *J. Appl. Phys.* (in press).
- [22] S. H. Joen, B. H. Park, J. Lee, B. Lee and S. Han, *Appl. Phys. Lett.* **89**, 042904 (2006).
- [23] G. Gerra, A. K. Tagantsev, N. Setter and K. Parlinski, *Phys. Rev. Lett.* **96**, 107603 (2006).
- [24] L. J. Sinnamon, R. M. Bowman and J. M. Gregg, *Appl. Phys. Lett.* **78**, 1724 (2001).
- [25] W.-J. Lee, H.-G. Kim and S.-G. Yoon, *J. Appl. Phys.* **80**, 5891 (1996).